

How Viable Is a QCD Axion near 10 MeV?

Sudhakantha Girmohanta, Shota Nakagawa, Yuichiro Nakai and Junxuan Xu

*Tsung-Dao Lee Institute, Shanghai Jiao Tong University,
No. 1 Lisuo Road, Pudong New Area, Shanghai, 201210, China
School of Physics and Astronomy, Shanghai Jiao Tong University,
800 Dongchuan Road, Shanghai, 200240, China*

There has been an attempt to revive the visible QCD axion at the 10 MeV scale assuming that it exclusively couples to the first-generation quarks and the electron. This variant of the QCD axion is claimed to remain phenomenologically viable, partly due to a clever model construction that induces tree-level pion-phobia and exploits uncertainties inherent in the chiral perturbation theory. We confront this model with the cosmological domain wall problem, the quality issue and constraints arising from the electron electric dipole moment. It is also pointed out that the gluon loop-generated axion-top coupling can provide a very large contribution to rare B -meson decays, such that the present LHCb data for $B^0 \rightarrow K^{*0} e^+ e^-$ rule out the model for the axion mass larger than 30 MeV. There is a strong motivation for pushing the experimental analysis of $B \rightarrow K^{(*)} e^+ e^-$ to a lower $e^+ e^-$ invariant mass window, which will conclusively determine the fate of the model, as its contribution to this branching ratio significantly exceeds the Standard Model prediction.

I. INTRODUCTION

The Standard Model (SM) has achieved incredible success in accounting for the experimental data observed to date, yet it leaves several theoretical issues unresolved. The strong CP problem, namely why the CP-violating parameter originating from the topological vacuum nature in QCD (θ) is smaller than $\sim 10^{-10}$, remains one of the outstanding puzzles.¹ As the viability of the massless up quark has been ruled out from the lattice simulations [2, 3], the most popular dynamical solution is due to Peccei and Quinn (PQ) where a global $U(1)_{\text{PQ}}$ symmetry is spontaneously broken, giving rise to a (pseudo-)Nambu-Goldstone boson a , the axion [4–6]. Once the axion settles down into the minimum of the potential induced by the strong interaction, the strong CP problem is dynamically solved.

The original visible QCD axion, with a decay constant f_a at the electroweak scale, was soon ruled out as a result of constraints from rare meson decays, and subsequently, attention was shifted to the invisible axion with a much larger f_a (and smaller mass) [7, 8]. Nevertheless, it has been claimed in Ref. [9] that the exclusion for the axion at the 10 MeV scale is not conclusive, and a particular pion-phobic variant, where the axion only couples to the first-generation quarks and the electron by model construction, can still be viable. This possibility is also motivated by the still indecisive claim of an $e^+ e^-$ excess in the ^8Be nuclear de-excitation spectrum [10].

Progress has been made toward achieving a realistic UV complete model of this QCD axion variant in Ref. [11], where the PQ symmetry breaking is intertwined with the electroweak symmetry breaking such that the observed CKM mixing matrix can be reproduced. It is valuable to consider the viability of a QCD axion in this mass range regardless of the indecisive experimental hints and confront it with current experimental and cosmological constraints and discuss possible future probes.

In the present paper, we discuss several new theoretical and experimental consequences of the aforementioned visible QCD axion. As the decay constant f_a is around GeV for the axion at the 10 MeV scale, the PQ symmetry breaking is likely to take place in the Universe after inflation. Further, since this variant necessarily couples to the first-generation quarks, the domain wall number is larger than 1. Hence, the PQ phase transition generates a string-domain wall network, which results in a catastrophic deviation from the standard cosmology unless it decays rapidly. The introduction of a sufficiently large bias term in the form of operators that explicitly break the PQ symmetry enables the network to decay. However, the strength of these operators must be suppressed enough not to spoil the quality of the PQ symmetry to achieve $\bar{\theta} \lesssim 10^{-10}$. We will study the interplay of these two conditions for the axion at the 10 MeV scale.

The $U(1)_{\text{PQ}}$ charge of the up and down quarks must be different to realize the required pion-phobia [12]. Therefore, in a renormalizable UV completion, one generically needs multiple additional Higgs doublets, inevitably introducing new CP-violating phases in the scalar potential. Working with the benchmark model in Ref. [11], we will present those CP-violating phases. Then, electric dipole moments (EDMs) are generated as a result of the new complex phases. We will find that the electron EDM

¹ It was noted however that, setting $\bar{\theta} = 0$ at some UV scale, the Cabibbo–Kobayashi–Maskawa (CKM) phase only generates $\bar{\theta} \sim 10^{-16}$ [1].

generated at one/two-loop in the model gives the most stringent constraint on the new physics mass scale.

Although the tree-level interactions of the visible axion to the higher generation quarks are zero by the model construction, they are generated via gluon loops. While these loop generated interactions to the b and c -quarks, constrained by the decays of J/Ψ and Υ , have been considered in the literature [9, 13], the similar coupling to the top quark was neglected, because we cannot produce the corresponding *topped* bound state, and the top quark decays even before it can hadronize. Here, however, we will argue that the axion-top coupling generated through a gluon loop gives a dominant new physics contribution to decays like $B \rightarrow Ka$ (see Refs. [14, 15] for constraints from searches of other ultra-rare K -decay modes induced by the QCD axion). In particular, as the present axion variant promptly decays to a e^+e^- pair to be consistent with the beam dump experiments, the rare decay mode $B^0 \rightarrow K^{*0}e^+e^-$ can be used to constrain the model. We show that the contribution of the visible QCD axion to the branching ratio of the decay is much larger than that of the SM. Then, the current LHCb data [16], applicable to the invariant mass of the e^+e^- pair in the range of 30-1000 MeV, rule out the model for the axion mass $m_a > 30$ MeV. We emphasize that there is a strong motivation for pushing the analysis for this mode into the lower invariant mass regime, which will conclusively determine the fate of the present visible axion variant.

The rest of the paper is organized as follows. In Sec. II, we briefly give a review of the QCD axion variant at the 10 MeV scale and its realistic UV completion. We discuss the quality and domain wall problems in Sec. III. Sec. IV deals with the induced electron EDM, while Sec. V discusses the constraints from the loop-mediated B -meson decay. Finally, we conclude in Sec. VI.

II. REVIEW OF QCD AXION NEAR 10 MEV

Let us begin with a review of the QCD axion variant with mass of $\mathcal{O}(10)$ MeV discussed in Refs. [9, 11, 13]. It had been widely believed that such a visible axion model can be easily excluded by beam dump experiments [17] or measurements of rare heavy meson decays [18, 19]. However, the authors of Ref. [9] claimed a possible way out of those severe constraints on the model, which is composed of three points: (i) the axion must couple to only the first-generation of the SM fermions, (ii) the axion is required to be pion-phobic [12], and (iii) there exist large uncertainties in theory and experiment. For point (i), only the axion couplings to the first-generation quarks (u, d) are allowed to avoid exotic decays of the heavy quarkonia, e.g. J/ψ and Υ [20–24]. The axion must couple to the electron as otherwise it would become too long-lived and would have been already detected by beam dump experiments (the lifetime is bounded as $\tau \lesssim 10^{-13}$ sec) [25–28]. The axion coupling to the muon is prohibited by the measurement of the muon magnetic dipole moment unless the

	H	H_u	H_d	H_e	Φ_u	Φ_d	Φ_e
$SU(2)_L$	2	2	2	2	1	1	1
$U(1)_Y$	1/2	-1/2	1/2	1/2	0	0	0
$U(1)_{PQ}$	0	$-Q_u$	$-Q_d$	$-Q_e$	$-Q_u$	$-Q_d$	$-Q_e$

TABLE I: The charge assignments of scalar fields.

decay constant f_a is larger than the electroweak scale. Regarding point (ii), pion-phobia enables the axion-pion mixing to be suppressed, leading to the tiny rate of an exotic decay of the pion. The SINDRUM collaboration [29] searches for the process $\pi^+ \rightarrow e^+\nu_e a (\rightarrow e^+e^-)$ and provides a constraint on the branching ratio, resulting in the upper bound on the axion-pion mixing. To realize pion-phobia, one can take special PQ charge assignments of u and d ,

$$\frac{Q_u}{Q_d} = 2, \quad (1)$$

leading to the cancellation due to the mass ratio between u and d . For point (iii), the axion- η meson mixing induces a $K^+ \rightarrow \pi^+ a$ decay, however, the inherent uncertainties in the chiral perturbation theory have been used to argue that the QCD axion variant remains viable [9]. Note that Eq. (1) only realizes tree-level pion-phobia, and the effective PQ charges receives corrections due to the renormalization group evolution (RGE) [30, 31]. For example, including the dominant contribution from a top-induced vertex correction, the effective PQ charges for the u, d becomes

$$\begin{aligned} Q_u^{(1)} &= Q_u^0 - 6 \left(\frac{y_t}{4\pi} \right)^2 \ln \left(\frac{\Lambda_{UV}}{\mu} \right), \\ Q_d^{(1)} &= Q_d^0 + 6 \left(\frac{y_t}{4\pi} \right)^2 \ln \left(\frac{\Lambda_{UV}}{\mu} \right), \end{aligned} \quad (2)$$

where the running from Λ_{UV} to low-energy scale μ is considered, and y_t is the Yukawa coupling for top, and $Q_u^0 = 2, Q_d^0 = 1$ are the tree-level PQ charge assignments. The resulting change in axion-pion mixing angle is less than its current uncertainty stemming from m_u/m_d measurement. Together with the uncertainties in the higher order chiral perturbation theory, pion-phobia can be realized including RGE effects, perhaps in a slightly different parameter space [32].

For other requirements, we should mention the bound from the electron magnetic moment, $(g-2)_e$. The axion-electron and -photon couplings induce loop contributions to $(g-2)_e$ and thus receive a constraint from the current measurements.² In addition, the axion coupling to

² There is a discrepancy of values of $(g-2)_e$ calculated by using values of the fine-structure constant measured by two independent experiments. While the cesium recoil experiment [33] leads to a smaller value of $(g-2)_e$, the experiment using the rubidium atom [34] leads to a larger value. The recent measurement of $(g-2)_e$ [35] does not solve the tension.

the electron is constrained by KLOE [36] and NA64 experiments [37, 38]. Taking account of both bounds, we obtain the allowed range of the PQ charge of the electron, $1/3 \lesssim Q_e \lesssim 2$.

We now consider a UV model to satisfy the requirements, following the discussion of Ref. [11]. The model introduces four doublet Higgs fields H, H_u, H_d, H_e and three SM-singlet scalar fields Φ_u, Φ_d, Φ_e . Here, H corresponds to the usual SM Higgs doublet. The charge assignments of these scalar fields are summarized in Tab. I, where we define the PQ charges of the right-handed up quark u_R , down quark d_R and electron e_R as Q_u, Q_d and Q_e , respectively. In the following discussion, we set them as

$$Q_u = 2, \quad Q_d = 1, \quad Q_e = \frac{1}{n}, \quad (3)$$

with $n = 2, 3$. This choice makes the axion pion-phobic and evades the bound on Q_e conservatively. The color anomaly is estimated as $(Q_u + Q_d)/2$, and the domain wall number is three. Yukawa interactions with the new Higgs doublets and the SM one are respectively given by

$$\begin{aligned} \mathcal{L}_{\text{PQ}}^Y &= - \sum_{i=1,2,3} (\bar{Q}^i Y_u^{i1} H_u u_R^1 + \bar{Q}^i Y_d^{i1} H_d d_R^1 \\ &+ \bar{L}^i Y_e^{i1} H_e e_R^1) + \text{h.c.}, \end{aligned} \quad (4)$$

$$\begin{aligned} \mathcal{L}_{\text{SM}}^Y &= - \sum_{i=1,2,3} \sum_{j=2,3} (\bar{Q}^i Y_u^{ij} \tilde{H} u_R^j + \bar{Q}^i Y_d^{ij} H d_R^j \\ &+ \bar{L}^i Y_e^{ij} H e_R^j) + \text{h.c.}, \end{aligned} \quad (5)$$

where Q, L respectively denote the left-handed quark and lepton, the indices i, j represent the generation and $\tilde{H} \equiv i\sigma_2 H^*$. The first Lagrangian involves the first generation right-handed fermions, while the second one is relevant only to the second and third generation right-handed fermions. With these Yukawa interactions, the CKM matrix can be derived successfully [11].

The potential terms of the scalar fields to break the electroweak and PQ symmetries include

$$\begin{aligned} V_{\text{PQ}} &= (A_1 H H_u \Phi_u^* + A_2 H H_d^\dagger \Phi_d + A_3 H_e H^\dagger \Phi_e^* \\ &+ A_4 \Phi_u^* \Phi_d^2 + A_5 \Phi_d^* \Phi_e^n) + \text{h.c.}, \end{aligned} \quad (6)$$

$$V_{\text{dia}} = \sum_{\Psi} -\mu_{\Psi} \Psi^\dagger \Psi + \lambda_{\Psi} (\Psi^\dagger \Psi)^2. \quad (7)$$

Here, $\Psi = H, H_u, H_d, H_e, \Phi_u, \Phi_d, \Phi_e$ and A_1, A_2, A_3, A_4 and μ_{Ψ} are the parameters with mass dimension one and two, respectively. The mass dimension of the parameter A_5 depends on the choice of n , and λ_{Ψ} is a dimensionless coupling. Although other PQ-symmetric operators can be written down, they are not relevant for the PQ mechanism and omitted here. However, in Sec. IV, we will show that such extra terms induce sizable contributions to EDMs. In terms of seven neutral pseudoscalars, $\vec{\Phi}^I = (h^I, -h_u^I, h_d^I, h_e^I, \phi_u^I, \phi_d^I, \phi_e^I)^T$ where we take $-h_u^I$ for

\tilde{H}_u whose charge is the same as that of $H_{d,e}$, the physical axion degree of freedom is written as

$$\begin{aligned} a &\simeq \frac{1}{\sqrt{\sum_f Q_f^2 (v_f^2 + v_{\Phi_f}^2)}} \left(- \sum_f (-1)^f Q_f v_f^2 / v, -Q_u v_u, \right. \\ &Q_d v_d, Q_e v_e, Q_u v_{\Phi_u}, Q_d v_{\Phi_d}, Q_e v_{\Phi_e} \left. \right) \vec{\Phi}^I \\ &\equiv \vec{G}_{\text{PQ}}^T \vec{\Phi}^I, \end{aligned} \quad (8)$$

where v ($\simeq 246$ GeV), $v_u, v_d, v_e, v_{\Phi_u}, v_{\Phi_d}, v_{\Phi_e}$ denote vacuum expectation values (VEVs) of $H, H_u, H_d, H_e, \Phi_u, \Phi_d$ and Φ_e , respectively, and $(-1)^f = +1$ for $f = d, e$ and $(-1)^f = -1$ for $f = u$. In estimating the prefactor, we have used $v_f \ll v$. The axion-fermion coupling is then given by

$$\begin{aligned} \mathcal{L}_{aff} &= \sum_{f=u,d,e} \frac{m_f}{v_a} Q_f i a \bar{f} \gamma_5 f \\ &- \frac{\sum_f (-1)^f Q_f v_f^2}{v^2} \sum_{F=2\text{nd},3\text{rd}} \frac{m_F}{v_a} i a \bar{F} \gamma_5 F, \end{aligned} \quad (9)$$

with the PQ breaking scale, $v_a \equiv \sqrt{\sum_f Q_f^2 (v_f^2 + v_{\Phi_f}^2)}$. Note that we have the axion couplings to the 2nd and 3rd generation fermions, but they are suppressed by $(v_f/v)^2$.³ In Sec. V, we will point out extra contributions to those couplings induced by gluon loops.

The five physical pseudoscalar bosons (other than the axion and the Nambu-Goldstone mode absorbed by the Z boson) need to be heavy enough to evade the current experimental searches. In Ref. [11], the authors take the magnitudes of the VEVs and the A -term coefficients as

$$\begin{aligned} A_4 &\gg A_{k(=1,2,3)} \simeq 20 \text{ GeV}, \\ v_{f(=u,d,e)} &\simeq 20 \text{ MeV}, \quad v_{\Phi_{f(=u,d,e)}} \simeq 1 \text{ GeV}. \end{aligned} \quad (10)$$

The value of v_{Φ_f} sets the PQ breaking scale to $\mathcal{O}(1)$ GeV ($m_a = \mathcal{O}(10)$ MeV). Then, the three pseudoscalars are approximately given by linear combinations of h_f^I s, and their masses are estimated as $A_k v v_{\Phi_f} / v_f \sim (300 \text{ GeV})^2$. Looking at the fourth term in Eq. (6), one massive mode is described as a linear combination of Φ_u and Φ_d , and its mass is given by $A_4 v_{\Phi_f} \gg (1 \text{ GeV})^2$. We can take a large value of A_4 to make this mode sufficiently heavy. For $n = 2$, A_5 is dimensionful, and hence the last pseudoscalar mode can be heavy by taking a large value of A_5 . On the other hand, for $n = 3$, A_5 is a dimensionless constant, so that the last mode has a relatively small mass of $A_5 v_{\Phi_f}^2 \sim (1 \text{ GeV})^2$. This mode is dominantly composed of Φ_e without other A -term interactions, and then

³ The axion coupling to the muon through Higgs mixing effects is tiny. Quantitatively, the axion contribution to muon magnetic moment $(g-2)_\mu \lesssim 10^{-20}$.

mainly couples to the electron. The coupling strength is estimated as $|Y_e|v_f/v_{\Phi_f} \simeq m_e/v_{\Phi_f} \simeq 5 \cdot 10^{-4}$, and constrained by dark photon searches, such as BaBar [39] for the mass range of 1 – 10 GeV. Hence, the case of $n = 3$ is marginally consistent with the current bound. In addition to those pseudoscalars, there are seven CP-even scalars in the model. First, we have the SM-like Higgs boson with mass-squared of $\sim \lambda_H v^2$. Then, as in the case of the pseudoscalar modes, three modes obtain masses of $\sim A_k v v_{\Phi_f}/v_f$ and two modes have masses of $\sim A_4 v_{\Phi_f}$. For $n = 2$, taking a large value of A_5 , all the CP-even scalars are sufficiently heavy. For $n = 3$, there remains a light mode whose mass is of $\mathcal{O}(1)$ GeV, and the similar experimental constraint as that of the pseudoscalar is applied to this mode.⁴ We assume the magnitudes of Eq. (10) in the following discussion.

III. QUALITY AND COSMOLOGY

The PQ mechanism can solve the strong CP problem dynamically under the assumption that the PQ symmetry is well preserved. However, the PQ symmetry is introduced as a global symmetry, and we naturally expect Planck-suppressed operators breaking the PQ symmetry explicitly [41–49]. For invisible axion models with large f_a , they destroy the PQ solution, which is known as the axion quality problem. Here, we discuss whether the similar problem exists or not in the visible axion model with $f_a = \mathcal{O}(1)$ GeV. We also explore a possibility that those PQ violating operators provide bias terms to solve the domain wall problem.

A. Explicit PQ breaking operators

For the visible QCD axion model presented in Sec. II, PQ-breaking higher-dimensional operators that are the most dangerous for the PQ solution are

$$\begin{aligned} \mathcal{L}_{\mathcal{PQ}} = & \sum_{f=u,d,e} \left(g_1 \frac{(HH^\dagger)^2 \Phi_f}{M_{\text{Pl}}} + g_2 \frac{HH^\dagger \Phi_f^3}{M_{\text{Pl}}} \right. \\ & \left. + g_3 \frac{\Phi_f^5}{M_{\text{Pl}}} + \dots \right) + \text{h.c.}, \end{aligned} \quad (11)$$

where each $g_i = |g_i|e^{i\delta_i}$ ($i = 1, 2, 3$) is a complex coupling constant with a phase shift δ_i and is assumed to be

independent of f for simplicity. Here, we have omitted to write down combinations such as $\Phi_u^3 \Phi_d^2$, which will be taken into account in the final results. The three terms in Eq. (11) respectively generate the following axion potential terms:

$$V_{\mathcal{PQ}}^{(1)} = -\frac{|g_1|}{2\sqrt{2}} \frac{v^4}{M_{\text{Pl}}} \sum_f v_{\Phi_f} \cos\left(Q_f \frac{a}{v_a} + \delta_1\right), \quad (12)$$

$$V_{\mathcal{PQ}}^{(2)} = -\frac{|g_2|}{2\sqrt{2}} \frac{v^2}{M_{\text{Pl}}} \sum_f v_{\Phi_f}^3 \cos\left(3Q_f \frac{a}{v_a} + \delta_2\right), \quad (13)$$

$$V_{\mathcal{PQ}}^{(3)} = -\frac{|g_3|}{2\sqrt{2}} \sum_f \frac{v_{\Phi_f}^5}{M_{\text{Pl}}} \cos\left(5Q_f \frac{a}{v_a} + \delta_3\right). \quad (14)$$

They shift the axion VEV from the CP conserving minimum, which is set by the potential from QCD nonperturbative effects, $V_a = m_a^2 f_a^2 (1 - \cos(a/f_a))$. Here the axion mass m_a is given by

$$m_a = \frac{\sqrt{m_u m_d}}{m_u + m_d} \frac{m_\pi f_\pi}{f_a}, \quad (15)$$

where the decay constant of the axion is defined as $f_a \equiv v_a/N_{\text{DW}}$ with domain wall number $N_{\text{DW}} (= Q_u + Q_d = 3)$, and $m_\pi \simeq 135$ MeV and $f_\pi \simeq 92$ MeV denote the pion mass and decay constant, respectively. For the term $V_{\mathcal{PQ}}^{(1)}$, the shift of the axion VEV is evaluated as

$$\frac{\langle a \rangle}{f_a} \simeq \frac{|g_1|}{2\sqrt{2}N_{\text{DW}}} \frac{v^4}{M_{\text{Pl}} m_a^2 f_a^2} \sum_f Q_f v_{\Phi_f} \sin \delta_1. \quad (16)$$

Those corresponding to $V_{\mathcal{PQ}}^{(2)}$ and $V_{\mathcal{PQ}}^{(3)}$ can be estimated similarly.

The current neutron EDM measurement provides an upper bound on $\bar{\theta}$ [50, 51], such that $\langle a \rangle / f_a \lesssim 10^{-10}$. This bound can be read out as upper bounds on the coupling coefficients $|g_i|$. Considering each operator as the dominant one, we obtain

$$|g_1| \lesssim 8 \times 10^{-6} \left(\frac{m_a}{10 \text{ MeV}} \right), \quad (17)$$

$$|g_2| \lesssim 0.03 \left(\frac{\Delta^{(2)}}{10} \right)^{-1} \left(\frac{3}{N_{\text{DW}}} \right)^2 \left(\frac{m_a}{10 \text{ MeV}} \right)^3, \quad (18)$$

$$|g_3| \lesssim 200 \left(\frac{\Delta^{(3)}}{100} \right)^{-1} \left(\frac{3}{N_{\text{DW}}} \right)^4 \left(\frac{m_a}{10 \text{ MeV}} \right)^5. \quad (19)$$

Here, we use $f_a \simeq \sqrt{\sum Q_f^2 v_{\Phi_f}^2} / N_{\text{DW}}$ and take $n = 2$ and $\delta_i = 1$. Since we expect $\mathcal{O}(10)$ and $\mathcal{O}(100)$ number of operators in Eq. (11) giving similar contributions to Eq. (13) and Eq. (14), respectively, the factors of $\Delta^{(2)} = \mathcal{O}(10)$ and $\Delta^{(3)} = \mathcal{O}(100)$ are included for the bounds on $|g_2|$ and $|g_3|$. The results show that fine-tuning of $\mathcal{O}(10^{-5})$ is required for the PQ quality in the presence of the coupling g_1 . The f_a (or m_a) dependence of bounds

⁴ The reported e^+e^- excess in the de-excitation of ^8Be and ^4He [10, 40] and $(g-2)_e$ can be simultaneously explained by this axion model for $n = 2, 3$ [11, 13], we mainly consider the case of $n = 2, 3$ in the present paper for comparison. However, as the uncertainty in fine structure measurements is larger than the uncertainty in $(g-2)_e$, disregarding the $(g-2)_e$ discrepancy explanation, the $n = 1$ case can be allowed, when the model can be more minimal, composed of five Higgs fields.

on $|g_i|$ is also summarized in Fig. 1. The results for $n = 3$ are not significantly different from those of $n = 2$.

While, compared to the invisible QCD axion models, the PQ quality for the visible axion at the 10 MeV scale is much better, the complete PQ quality requires removal of higher-dimensional operators involving the SM Higgs. This conclusion comes from the fact that the PQ breaking scale is below the electroweak scale. A small axion decay constant is not sufficient to achieve the high quality of the PQ symmetry. However, this issue might be addressed by a further model-building.

B. Domain wall problem

Spontaneous breaking of the PQ symmetry after inflation generates topological defects which can give a non-negligible impact on the evolution of the Universe. At the PQ phase transition, cosmic strings are formed through the Kibble mechanism [53, 54], and when the axion acquires a potential from nonperturbative effects of QCD, domain walls are produced and the string-wall system appears. Its cosmological consequence depends on the domain wall number N_{DW} of a model. If $N_{\text{DW}} = 1$, the string-wall system is unstable and collapses with a short lifetime. On the other hand, if $N_{\text{DW}} > 1$, it is stable and may quickly dominate the Universe. This is known as the cosmological domain wall problem (see Refs. [55, 56] for recent reviews). One possible solution to the domain wall problem is to introduce an explicit PQ breaking operator (often called bias term), which lifts up the degenerate vacua and makes the string-wall system unstable [57–59]. However, for invisible axion models, the solution is in tension with the quality of the PQ symmetry, and one has to adjust the axion potential from the explicit breaking operator so that its minimum is aligned with that of the potential from nonperturbative effects of QCD [60].

The situation is improved considerably for the visible axion model with $f_a = \mathcal{O}(1)$ GeV. In order to solve the domain wall problem, it is sufficient to find a condition that the domain wall collapses through a PQ-breaking operator before the Big Bang Nucleosynthesis (BBN) so as not to destroy the light elements. The PQ-breaking operator makes an energy difference ΔV between the vacua, which induces a volume pressure on the domain wall. The wall becomes unstable when the volume pressure is comparable to the domain wall tension:

$$\Delta V \sim \frac{\beta \sigma_{\text{wall}}}{t_{\text{dec}}}. \quad (20)$$

Here, $\sigma_{\text{wall}} \simeq 9.25 m_a f_a^2$ is the surface density of the domain wall [61, 62], β is a constant which is $\mathcal{O}(1)$ by dimensional analysis, and t_{dec} is the cosmic time when the domain wall decays. The potential difference between the origin and its neighbor vacuum is approximately given by

$$\Delta V \sim |V_{\text{PQ}}(a = 2\pi v_a / N_{\text{DW}}) - V_{\text{PQ}}(0)|. \quad (21)$$

For $V_{\text{PQ}}^{(3)}$ in Eq. (14), the constraint from the domain wall lifetime is shown in the blue shaded region of the right panel of Fig. 1. Although we take $n = 2$ here, a similar result can be obtained for $n = 3$. We can see that the constraint is still satisfied without causing the axion quality problem. For $V_{\text{PQ}}^{(1,2)}$ in Eqs. (12), (13), the domain wall decays even faster, and the constraint does not appear in the left panel of Fig. 1 although there is a quality issue for those operators. In conclusion, if we can somehow suppress higher-dimensional operators involving the SM Higgs which lead to $V_{\text{PQ}}^{(1,2)}$ but allow the third term of Eq. (11) leading to Eq. (14) by model-building, the domain wall problem is solved with the high-quality of the PQ symmetry.

IV. ELECTRON EDM

The model contains three Higgs doublet fields H_f ($f = u, d, e$) and SM-singlet scalars Φ_f as well as the SM Higgs field. According to the charge assignment summarized in Tab. I, many scalar potential terms other than those presented in Eqs. (6), (7) are actually allowed by the SM gauge and PQ global symmetries. In the case of $n = 2$, all the possible (off-diagonal) scalar potential terms are

$$\begin{aligned} V_{\text{scalar}}^{(n=2)} = & A_1 H H_u \Phi_u^* + A_2 H H_d^\dagger \Phi_d + A_3 H_e H^\dagger \Phi_e^* \\ & + A_4 \Phi_u^* \Phi_d^2 + A_5 \Phi_d^* \Phi_e^2 + A_6 H_d H_e^\dagger \Phi_e^* \\ & + B_1 H H_u \Phi_d^{*2} + B_2 H H_d^\dagger \Phi_u \Phi_d^* + B_3 H H_d^\dagger \Phi_e^2 \\ & + B_4 H^\dagger H_e \Phi_d^* \Phi_e + B_5 H_u H_e \Phi_u^* \Phi_e^* + B_6 H_u H_d \Phi_u^* \Phi_d^* \\ & + B_7 H_d^\dagger H_e \Phi_d \Phi_e^* + B_8 \Phi_u \Phi_d^* \Phi_e^{*2} + B_9 H_e^2 H^\dagger H_d^\dagger \\ & + \text{h.c.}, \end{aligned} \quad (22)$$

where A_j ($j = 1, 2, \dots, 6$) and B_k ($k = 1, 2, \dots, 9$) are parameters with mass dimension one and dimensionless coupling constants, respectively. All the Higgs doublets and singlets get VEVs. Those parameters and VEVs are generally complex. Field redefinition rotates away some of the phases but is not sufficient to remove all, leading to observable phases.

The physical complex phases violate CP symmetry and lead to EDMs. Fig. 2a describes a one-loop diagram generating the electron EDM. The diagram includes the interactions, $A_3^* H_e^\dagger H \Phi_e$ and $B_4^* H H_e^\dagger \Phi_d \Phi_e^*$. The contribution to the electron EDM is then estimated as

$$\frac{d_e}{e} \sim \frac{\theta}{16\pi^2} |A_3^* B_4^* v^2 v_{\Phi_d}| \frac{m_e}{M^6}. \quad (23)$$

Here, θ and M denote the relevant physical phase and a representative mass scale of particles in the loop, respectively. The current experimental upper limit on the electron EDM is $d_e \leq 4.1 \times 10^{-30} e \text{ cm}$ [63]. With our choice of Eq. (10), the constraint can be satisfied for the mass scale,

$$M \gtrsim 500 \text{ GeV}, \quad (24)$$

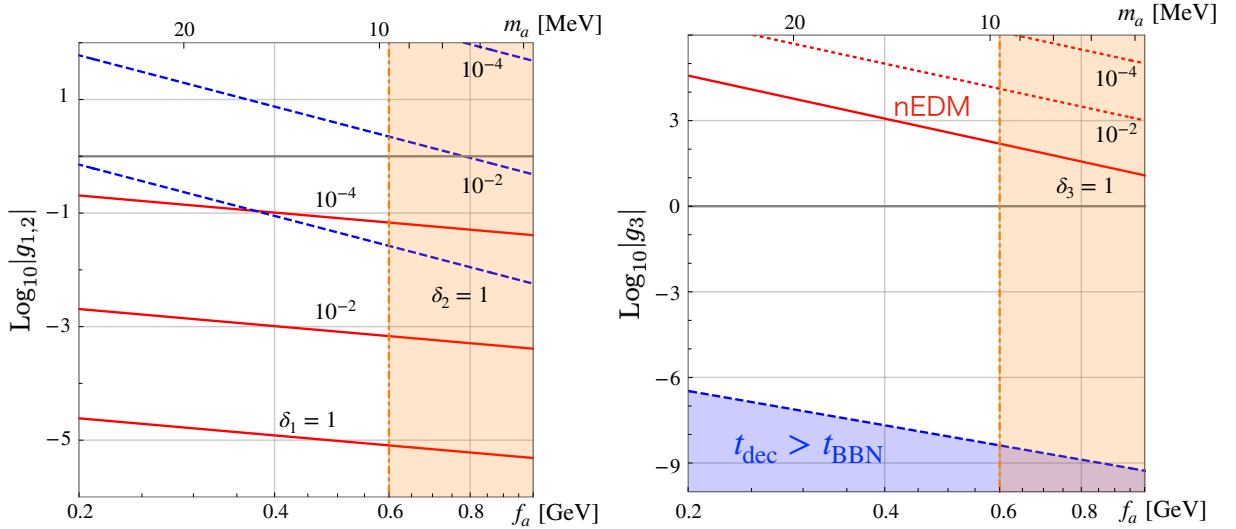


FIG. 1: *Left panel* : upper bounds on the coupling constants $|g_{1,2}|$ from the neutron EDM measurement as functions of f_a (lower axis) or m_a (upper axis) for the case of $n = 2$. The red solid and blue dashed lines represent the cases of $\delta_{1,2} = 1, 10^{-2}, 10^{-4}$ for Eq. (12) and Eq. (13), respectively. *Right panel* : bounds on the coupling constant $|g_3|$ of Eq. (14) from the neutron EDM measurement for $n = 2$. The red solid and dotted lines denote the bounds for $\delta_3 = 1, 10^{-2}, 10^{-4}$. In the blue shaded region, the domain wall survives after BBN. In both panels, the orange shaded regions are excluded by beam dump experiments [52].

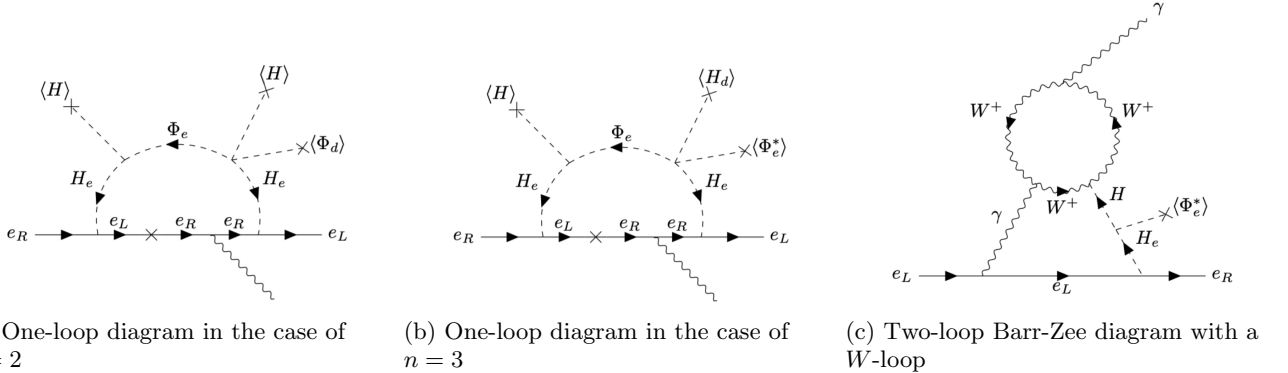


FIG. 2: Feynman diagrams for dominant contributions to the electron EDM. The arrows in the diagram represent charge flow.

where we have assumed the phase θ and the dimensionless coupling B_4 are of order one. As we have seen in Sec. II, all the (pseudo-)scalar particles inside the loop can have masses of $\mathcal{O}(100)$ GeV in the case of $n = 2$. Therefore, the condition (24) is marginally satisfied.

In the case of $n = 3$, the possible (off-diagonal) scalar potential terms allowed by the symmetries are

$$\begin{aligned}
 V_{\text{scalar}}^{(n=3)} = & A_1 H H_u \Phi_u^* + A_2 H H_d^\dagger \Phi_d + A_3 H_e H^\dagger \Phi_e^* \\
 & + A_4 \Phi_u^* \Phi_d^2 + A_5' \Phi_d^* \Phi_e^3 + B_1 H H_u \Phi_d^{*2} \\
 & + B_2 H H_d^\dagger \Phi_u \Phi_d^* + B_5 H_u H_e \Phi_u^* \Phi_e^* + B_6 H_u H_d \Phi_u^* \Phi_d^* \\
 & + B_7 H_d^\dagger H_e \Phi_d \Phi_e^* + B_{10} H_d H_e^\dagger \Phi_e^{*2} + \text{h.c.}, \quad (25)
 \end{aligned}$$

where A_5' and B_{10} denote dimensionless coupling constants. The diagram shown in Fig. 2b contains the inter-

actions, $A_3^* H_e^\dagger H \Phi_e$ and $B_{10} H_d H_e^\dagger \Phi_e^{*2}$. The contribution to the electron EDM is then estimated as

$$\frac{d_e}{e} \sim \frac{\delta}{16\pi^2} |A_3^* B_{10} v v_d v_{\Phi_e^*}| \frac{m_e}{M^6}, \quad (26)$$

with a relevant physical phase δ . The experimental upper limit can be satisfied for

$$M \gtrsim 100 \text{ GeV}. \quad (27)$$

Compared to the case of $n = 2$, the lower bound on the mass scale M becomes weaker. However, as described in Sec. II, the mass of Φ_e in the loop is typically $\mathcal{O}(1)$ GeV in the case of $n = 3$. Hence, it is likely that some fine-tuning in CP-violating phases is required to satisfy the EDM constraint. A more precise numerical estimate for the amount of tuning is left for a future study.

In addition to the one-loop contributions, a two-loop diagram with a fewer number of small VEV insertions may lead to a sizable contribution to the electron EDM. Fig. 2c describes a two-loop Bar-Zee-type diagram with inner W -loop. The diagram involves the CP-violating interaction $A_3 H_e H^\dagger \Phi_e^*$, and its contribution to the electron EDM is estimated as [64] (the general formula for a two-loop Bar-Zee-type diagram has been presented in Ref. [65] (see also Ref. [66]))

$$\frac{d_e}{e} \sim \frac{\alpha_e \zeta}{(4\pi)^3} \sqrt{2} G_F m_e \left(3f \left(\frac{m_W^2}{m_H^2} \right) + 5g \left(\frac{m_W^2}{m_H^2} \right) \right) \times \left| \frac{A_3 v_{\Phi_e}^*}{2\sqrt{2} M^2} \right| (\sin^2 \beta \tan \beta), \quad (28)$$

where α_e and G_F denote the fine-structure constant and Fermi coupling constant, respectively, ζ is the relevant physical phase and

$$f(z) \equiv \frac{1}{2} z \int_0^1 dx \frac{1-2x(1-x)}{x(1-x)-z} \ln \left(\frac{x(1-x)}{z} \right),$$

$$g(z) \equiv \frac{1}{2} z \int_0^1 dx \frac{1}{x(1-x)-z} \ln \left(\frac{x(1-x)}{z} \right).$$

The parameter β is defined as

$$\tan \beta \equiv \frac{v}{v_e} \sim 10^4. \quad (29)$$

The experimental constraint can be satisfied for

$$M \gtrsim 8 \text{ TeV}, \quad (30)$$

which gives a stronger bound (independent of the value of Q_e), compared to those of the one-loop contributions. Fine-tuning in CP-violating phases and/or some mechanism to suppress the phases are necessary.

In addition to the electron EDM constraint, we are able to consider those of the neutron EDM [50] and mercury EDM [67] where the chromo-EDM of the down quark and the electron EDM give main contributions. The resulting constraints are found to be weaker than the one directly given by the electron EDM measurement.

V. LOOP INDUCED B-DECAY

To evade stringent constraints from rare decay modes of heavy mesons such as B , Υ mediated by the QCD axion variant under consideration, it has been assumed that the axion only couples to the first-generation quarks u , d , and to the electron at the tree level. However, from a UV completion perspective, the PQ symmetry breaking, together with the electroweak symmetry breaking, has to generate the observed CKM mixing matrix. Therefore, inevitably, couplings of the axion to heavier generation quarks will be generated via mixing with the SM Higgs. Progress towards understanding this has been made in

Ref. [11], where a hierarchy between the VEVs of additional Higgses and the SM Higgs has been deemed to suppress the axion couplings to the 2nd and 3rd generation quarks to $\sim \mathcal{O}(10^{-7})$ level.

Here we point out that a gluon loop will also induce the axion couplings to the heavier quarks. Namely,

$$\mathcal{L}_{aFF} = Q_{F,\text{eff}}^{\text{PQ}} \frac{m_F}{v_a} a \bar{F} i \gamma_5 F,$$

$$Q_{F,\text{eff}}^{\text{PQ}} \simeq C_F \left(\frac{\alpha_s}{4\pi} \right)^2, \quad (31)$$

where F can be any 2nd or 3rd generation quark, and $C_F = 4/3$ is the quadratic Casimir, and α_s is the strong coupling constant. The two-loop suppression effect in Eq. (31) comes from the fact that the axion-gluon coupling inherits a loop factor, generated through the up and down quarks flowing in the triangle anomaly diagrams. Furthermore, the anomalous dimension of this coupling is $-6C_F(\alpha_s/4\pi)^2$, and it is not changed significantly upon running. Therefore, the 1-loop gluon-induced coupling to the bottom quark is $Q_{b,\text{eff}}^{\text{PQ}} \simeq 3 \times 10^{-4}$, where we have used the running coupling α_s relevant for the process $\Upsilon \rightarrow \gamma a$, which requires $Q_{b,\text{eff}}^{\text{PQ}} \lesssim 0.8 \times 10^{-2}$ [9]. Hence, the 1-loop gluon-generated coupling to the b quark is consistent with bounds from rare Υ decays.

Let us now consider the loop-mediated decays of the B -meson such as $B \rightarrow Ka$. This is obtained by integrating out the W -loop as in Fig. 3. The effective b - s - a vertex is denoted as

$$\mathcal{L}_{bsa} = -ig_{bsa} \bar{s}_L b_R a + \text{h.c.}, \quad (32)$$

where we utilized the chirality-flipping nature of the diagram to infer that the coefficient of $\bar{s}_R b_L$ is suppressed as m_s/m_b . The leading-log result is well-known [68],

$$g_{bsa} = \frac{G_F m_W^2}{4\sqrt{2}\pi^2} \frac{m_b}{v_a} \sum_{u_i=u,c,t} Q_{u_i,\text{eff}}^{\text{PQ}} \frac{m_{u_i}^2}{m_W^2} V_{u_i s} V_{u_i b} \ln \left(\frac{\Lambda_{\text{UV}}^2}{m_{u_i}^2} \right), \quad (33)$$

where we have included a summation over all the up-type quarks, with an effective coupling to the higher generation understood as given in Eq. (31), and Λ_{UV} is taken as the UV cut-off of the theory. Although the top-axion coupling is loop generated, it contributes dominantly to g_{bsa} as evident in Eq. (33). To be consistent with the beam dump decay experiment, the axion should decay into an e^+e^- pair with lifetime $\tau_a \lesssim 10^{-13}$ s. Hence, we employ the experimental measurement on the branching ratio of the rare decay mode $B^0 \rightarrow K^{*0} e^+ e^-$ by LHCb [16, 69],⁵

$$\mathcal{B}(B^0 \rightarrow K^{*0} e^+ e^-) = (3.1_{-0.8}^{+0.9+0.2} \pm 0.2(\mathcal{B})) \times 10^{-7}. \quad (34)$$

⁵ Here the errors are respectively statistical, systematic, and relating to the uncertainties on the $B^0 \rightarrow J/\Psi K^{*0}$ and $J/\Psi \rightarrow e^+e^-$ branching fractions, which were used as normalization channels.

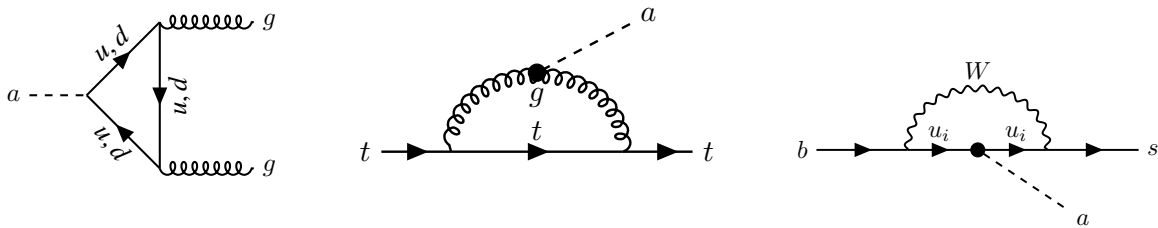


FIG. 3: Feynman diagrams that generate the axion couplings to gluons and the top quark, mediating the B -meson decay.

Note that this measurement is only applicable for dilepton invariant mass in the range of 30-1000 MeV, which is slightly higher than the axion mass we are interested in, however, it should be noted that the theoretical expectation from the SM is not very sensitive to the dilepton invariant mass, and can be predicted up to the order one logarithmic correction factor as [70]

$$\mathcal{B}^{\text{SM}}(B^0 \rightarrow K^{*0} e^+ e^-) \simeq 2.43_{-0.47}^{+0.66} \times 10^{-7}. \quad (35)$$

Given the axion coupling in Eq. (32), the BSM contribution can be written as

$$\begin{aligned} \mathcal{B}^{\text{BSM}}(B^0 \rightarrow K^{*0} e^+ e^-) \\ = \frac{|g_{bsa}|^2}{16\pi m_B \Gamma_B} \lambda_{B,K^*a}^{1/2} |\langle K^* | \bar{s}_L b_R | B \rangle|^2, \end{aligned} \quad (36)$$

where

$$\lambda_{x,yz} \equiv \left[1 - \left(\frac{m_y}{m_x} - \frac{m_z}{m_x} \right)^2 \right] \left[1 - \left(\frac{m_y}{m_x} + \frac{m_z}{m_x} \right)^2 \right],$$

$$|\langle K^* | \bar{s}_L b_R | B \rangle|^2 = \frac{1}{4} \frac{m_B^4 \lambda_{B,K^*a}}{(m_b + m_s)^2} [\mathcal{A}_{K^*}(m_a^2)]^2, \quad (37)$$

$$\mathcal{A}_{K^*}(q^2) = \frac{1.36}{1 - q^2/27.9 \text{ GeV}^2} - \frac{0.99}{1 - q^2/36.8 \text{ GeV}^2}.$$

The pion-phobic QCD axion variant, which by an ad-hoc model construction only couples to the first-generation quarks at the tree level, when considered together with the gluon loop generated coupling to the top quark, can mediate the B -decay with a contribution much larger than that of the SM. For numerical illustration, taking $m_a = 10$ MeV, we find

$$\frac{\mathcal{B}^{\text{BSM}}(B^0 \rightarrow K^{*0} a(\rightarrow e^+ e^-))}{\mathcal{B}^{\text{SM}}(B^0 \rightarrow K^{*0} e^+ e^-)} \simeq 10^3 \ln \left(\frac{\Lambda_{\text{UV}}}{m_t} \right)^2, \quad (38)$$

where we have used the QCD relation in Eq. (15) together with $v_a = N_{\text{DW}} f_a$ for this model, which fixes $v_a \simeq 1.7$ GeV for $m_a = 10$ MeV. This BSM contribution to the rare meson decay increases with increasing m_a , as the corresponding v_a decreases. Hence, in light of the LHCb analysis [16, 69], the pion-phobic QCD axion variant is ruled out for $m_a > 30$ MeV mass range.

The current most precise measurement of the branching ratio for $B \rightarrow K^{(*)} e^+ e^-$ comes from Belle [71] and

BaBar [72] collaborations. However, they used a veto of $q^2 \lesssim 0.1 \text{ GeV}^2/c^4$ to reduce the background. Therefore, we cannot use their result to constrain the axion mass below ~ 300 MeV. We note that below 30 MeV dilepton invariant mass, multiple scatterings obscure the angular analysis of the outgoing electrons in $B^0 \rightarrow K^{*0} e^+ e^-$, however, if one is only interested in searching for this mode without the angular correlation, the background contamination only comes from the photon converting to $e^+ e^-$ in the mode $B^0 \rightarrow K^{*0} \gamma$. It is also conceivable that meaningful constraints can be obtained by analyzing the off-shell contribution of this axion variant to the lower dilepton mass bins. Hence, there is a strong motivation for the LHCb and Belle II experiments to make an updated analysis and push the search for this mode towards the lower end of the dilepton invariant mass from 30 MeV down to a few MeV that will determine the fate of the model conclusively.

VI. CONCLUSIONS

We have considered new theoretical and phenomenological constraints on the $\mathcal{O}(10)$ MeV pion-phobic QCD axion variant that has been argued to be still viable [9]. Due to the very low PQ breaking scale, the phase transition takes place after inflation, and the string-domain wall network is formed. We have investigated the interplay of the lifetime of the network and the quality issue of the PQ symmetry due to a necessary bias term. It was found that an appropriate choice of a higher-dimensional operator by some model-building can solve the domain wall problem with the high-quality of the PQ symmetry. From a UV completion perspective, as the PQ charges of the up and down quarks and electron have to be different in the model, one has to introduce multiple new scalar fields. This brings the model a plethora of new CP-violating terms that manifest themselves as EDMs. We have identified the dominant electron EDM contribution and analyzed the resulting constraints. Finally, we have pointed out that the gluon loop-induced top-quark coupling of the axion contributes to rare B -decay modes, and in particular to $B \rightarrow K^{(*)} a(\rightarrow e^+ e^-)$ for the current axion model. Experimental data for this mode already exclude the model for the axion mass larger than 30 MeV. There is a strong motivation for pushing the

experimental analysis to a lower dilepton mass window by the LHCb and Belle collaborations, which will dictate the fate of the model.

ACKNOWLEDGMENTS

We thank Chia-Wei Liu and Yoshihiro Shigekami for useful discussions.

-
- [1] J. R. Ellis and M. K. Gaillard, *Nucl. Phys. B* **150**, 141 (1979).
- [2] R. L. Workman *et al.* (Particle Data Group), *PTEP* **2022**, 083C01 (2022).
- [3] C. Alexandrou, J. Finkenrath, L. Funcke, K. Jansen, B. Kostrzewa, F. Pittler, and C. Urbach, *Phys. Rev. Lett.* **125**, 232001 (2020), arXiv:2002.07802 [hep-lat].
- [4] R. D. Peccei and H. R. Quinn, *Phys. Rev. Lett.* **38**, 1440 (1977).
- [5] S. Weinberg, *Phys. Rev. Lett.* **40**, 223 (1978).
- [6] F. Wilczek, *Phys. Rev. Lett.* **40**, 279 (1978).
- [7] J. E. Kim, *Phys. Rev. Lett.* **43**, 103 (1979).
- [8] M. Dine, W. Fischler, and M. Srednicki, *Phys. Lett. B* **104**, 199 (1981).
- [9] D. S. M. Alves and N. Weiner, *JHEP* **07**, 092 (2018), arXiv:1710.03764 [hep-ph].
- [10] A. J. Krasznahorkay *et al.*, *Phys. Rev. Lett.* **116**, 042501 (2016), arXiv:1504.01527 [nucl-ex].
- [11] J. Liu, N. McGinnis, C. E. M. Wagner, and X.-P. Wang, *JHEP* **05**, 138 (2021), arXiv:2102.10118 [hep-ph].
- [12] L. M. Krauss and D. J. Nash, *Phys. Lett. B* **202**, 560 (1988).
- [13] D. S. M. Alves, *Phys. Rev. D* **103**, 055018 (2021), arXiv:2009.05578 [hep-ph].
- [14] M. Hostert and M. Pospelov, *Phys. Rev. D* **105**, 015017 (2022), arXiv:2012.02142 [hep-ph].
- [15] E. Cortina Gil *et al.* (NA62), *Phys. Lett. B* **846**, 138193 (2023), arXiv:2307.04579 [hep-ex].
- [16] R. Aaij *et al.* (LHCb), *JHEP* **05**, 159 (2013), arXiv:1304.3035 [hep-ex].
- [17] T. W. Donnelly, S. J. Freedman, R. S. Lytel, R. D. Peccei, and M. Schwartz, *Phys. Rev. D* **18**, 1607 (1978).
- [18] F. Wilczek, *Phys. Rev. Lett.* **39**, 1304 (1977).
- [19] L. J. Hall and M. B. Wise, *Nucl. Phys. B* **187**, 397 (1981).
- [20] H. Albrecht *et al.* (ARGUS), *Phys. Lett. B* **179**, 403 (1986).
- [21] S. Y. Hsueh and S. Palestini, *Phys. Rev. D* **45**, R2181 (1992).
- [22] T. A. Armstrong *et al.* (E760), *Phys. Rev. D* **47**, 772 (1993).
- [23] J. Z. Bai *et al.* (BES), *Phys. Lett. B* **355**, 374 (1995), [Erratum: *Phys.Lett.B* 363, 267 (1995)].
- [24] G. S. Adams *et al.* (CLEO), *Phys. Rev. D* **73**, 051103 (2006), arXiv:hep-ex/0512046.
- [25] F. Bergsma *et al.* (CHARM), *Phys. Lett. B* **157**, 458 (1985).
- [26] J. D. Bjorken, S. Ecklund, W. R. Nelson, A. Abashian, C. Church, B. Lu, L. W. Mo, T. A. Nunamaker, and P. Rassmann, *Phys. Rev. D* **38**, 3375 (1988).
- [27] M. Davier and H. Nguyen Ngoc, *Phys. Lett. B* **229**, 150 (1989).
- [28] J. Blumlein *et al.*, *Z. Phys. C* **51**, 341 (1991).
- [29] R. Eichler *et al.* (SINDRUM), *Phys. Lett. B* **175**, 101 (1986).
- [30] M. Chala, G. Guedes, M. Ramos, and J. Santiago, *Eur. Phys. J. C* **81**, 181 (2021), arXiv:2012.09017 [hep-ph].
- [31] M. Bauer, M. Neubert, S. Renner, M. Schnubel, and A. Thamm, *JHEP* **04**, 063 (2021), arXiv:2012.12272 [hep-ph].
- [32] L. Di Luzio, F. Mescia, E. Nardi, and S. Okawa, *Phys. Rev. D* **106**, 055016 (2022), arXiv:2205.15326 [hep-ph].
- [33] R. H. Parker, C. Yu, W. Zhong, B. Estey, and H. Müller, *Science* **360**, 191 (2018), arXiv:1812.04130 [physics.atom-ph].
- [34] L. Morel, Z. Yao, P. Cladé, and S. Guellati-Khélifa, *Nature* **588**, 61 (2020).
- [35] X. Fan, T. G. Myers, B. A. D. Sukra, and G. Gabrielse, *Phys. Rev. Lett.* **130**, 071801 (2023), arXiv:2209.13084 [physics.atom-ph].
- [36] A. Anastasi *et al.*, *Phys. Lett. B* **750**, 633 (2015), arXiv:1509.00740 [hep-ex].
- [37] D. Banerjee *et al.* (NA64), *Phys. Rev. D* **101**, 071101 (2020), arXiv:1912.11389 [hep-ex].
- [38] E. Depero *et al.* (NA64), *Eur. Phys. J. C* **80**, 1159 (2020), arXiv:2009.02756 [hep-ex].
- [39] J. P. Lees *et al.* (BaBar), *Phys. Rev. Lett.* **113**, 201801 (2014), arXiv:1406.2980 [hep-ex].
- [40] A. J. Krasznahorkay *et al.*, (2019), arXiv:1910.10459 [nucl-ex].
- [41] M. Dine and N. Seiberg, *Nucl. Phys. B* **273**, 109 (1986).
- [42] S. M. Barr and D. Seckel, *Phys. Rev. D* **46**, 539 (1992).
- [43] M. Kamionkowski and J. March-Russell, *Phys. Lett. B* **282**, 137 (1992), arXiv:hep-th/9202003.
- [44] M. Kamionkowski and J. March-Russell, *Phys. Rev. Lett.* **69**, 1485 (1992), arXiv:hep-th/9201063.
- [45] R. Holman, S. D. H. Hsu, T. W. Kephart, E. W. Kolb, R. Watkins, and L. M. Widrow, *Phys. Lett. B* **282**, 132 (1992), arXiv:hep-ph/9203206.
- [46] R. Kallosh, A. D. Linde, D. A. Linde, and L. Susskind, *Phys. Rev. D* **52**, 912 (1995), arXiv:hep-th/9502069.
- [47] L. M. Carpenter, M. Dine, and G. Festuccia, *Phys. Rev. D* **80**, 125017 (2009), arXiv:0906.1273 [hep-th].
- [48] L. M. Carpenter, M. Dine, G. Festuccia, and L. Ubaldi, *Phys. Rev. D* **80**, 125023 (2009), arXiv:0906.5015 [hep-th].
- [49] S. Girmohanta, Y.-C. Qiu, J.-W. Wang, and T. T. Yanagida, *Phys. Rev. D* **108**, 015028 (2023), arXiv:2303.02852 [hep-ph].

- [50] C. A. Baker *et al.*, *Phys. Rev. Lett.* **97**, 131801 (2006), [arXiv:hep-ex/0602020](#).
- [51] J. M. Pendlebury *et al.*, *Phys. Rev. D* **92**, 092003 (2015), [arXiv:1509.04411 \[hep-ex\]](#).
- [52] E. M. Riordan *et al.*, *Phys. Rev. Lett.* **59**, 755 (1987).
- [53] T. W. B. Kibble, *J. Phys. A* **9**, 1387 (1976).
- [54] T. W. B. Kibble, G. Lazarides, and Q. Shafi, *Phys. Rev. D* **26**, 435 (1982).
- [55] K. A. Beyer and S. Sarkar, *SciPost Phys.* **15**, 003 (2023), [arXiv:2211.14635 \[hep-ph\]](#).
- [56] M. Dine, (2023), [arXiv:2307.04710 \[hep-ph\]](#).
- [57] A. Vilenkin, *Phys. Rev. D* **23**, 852 (1981).
- [58] G. B. Gelmini, M. Gleiser, and E. W. Kolb, *Phys. Rev. D* **39**, 1558 (1989).
- [59] S. E. Larsson, S. Sarkar, and P. L. White, *Phys. Rev. D* **55**, 5129 (1997), [arXiv:hep-ph/9608319](#).
- [60] M. Kawasaki, K. Saikawa, and T. Sekiguchi, *Phys. Rev. D* **91**, 065014 (2015), [arXiv:1412.0789 \[hep-ph\]](#).
- [61] M. C. Huang and P. Sikivie, *Phys. Rev. D* **32**, 1560 (1985).
- [62] T. Hiramatsu, M. Kawasaki, K. Saikawa, and T. Sekiguchi, *JCAP* **01**, 001 (2013), [arXiv:1207.3166 \[hep-ph\]](#).
- [63] T. S. Roussy, L. Caldwell, T. Wright, W. B. Cairncross, Y. Shagam, K. B. Ng, N. Schlossberger, S. Y. Park, A. Wang, J. Ye, and E. A. Cornell, *Science* **381**, 46–50 (2023).
- [64] S. M. Barr and A. Zee, *Phys. Rev. Lett.* **65**, 21 (1990), [Erratum: *Phys.Rev.Lett.* 65, 2920 (1990)].
- [65] Y. Nakai and M. Reece, *JHEP* **08**, 031 (2017), [arXiv:1612.08090 \[hep-ph\]](#).
- [66] C. Cesarotti, Q. Lu, Y. Nakai, A. Parikh, and M. Reece, *JHEP* **05**, 059 (2019), [arXiv:1810.07736 \[hep-ph\]](#).
- [67] B. Graner, Y. Chen, E. Lindahl, and B. Heckel, *Physical Review Letters* **116** (2016), 10.1103/physrevlett.116.161601.
- [68] B. Batell, M. Pospelov, and A. Ritz, *Phys. Rev. D* **83**, 054005 (2011), [arXiv:0911.4938 \[hep-ph\]](#).
- [69] R. Aaij *et al.* (LHCb), *JHEP* **04**, 064 (2015), [arXiv:1501.03038 \[hep-ex\]](#).
- [70] S. Jäger and J. Martin Camalich, *JHEP* **05**, 043 (2013), [arXiv:1212.2263 \[hep-ph\]](#).
- [71] J. T. Wei *et al.* (Belle), *Phys. Rev. Lett.* **103**, 171801 (2009), [arXiv:0904.0770 \[hep-ex\]](#).
- [72] B. Aubert *et al.* (BaBar), *Phys. Rev. Lett.* **102**, 091803 (2009), [arXiv:0807.4119 \[hep-ex\]](#).